JACS ARTICLES

Published on Web 08/03/2010

Spectral−Structural Effects of the Keto−Enol−Enolate and Phenol−Phenolate Equilibria of Oxyluciferin

Panče Naumov* and Manoj Kochunnoonny

Department of Material and Life Science, Graduate School of Engineering, Osaka University, 2-1 Yamada-oka, Suita 565-0871, Osaka, Japan

Received April 6, 2010; E-mail: npance@wakate.frc.eng.osaka-u.ac.jp

Abstract: The effects of environmental polarity on the enolization of the keto form and the deprotonation of the enol, and the role of the neutral and ionized 6′-OH group in the fluorescence of the firefly emitter, oxyluciferin, were assessed through a detailed study of the structure and absorption and fluorescence spectra of its 6′-dehydroxylated analogue. It was found that the deprotonated 6′-O^- group is a necessary, albeit insufficient, factor in accounting for the observed yellow-green and red emissions of oxyluciferin. Its negative charge is essential for effective excited-state charge transfer, which lowers the emission energy and broadens the emission spectrum. Deprotonation of the 6′-OH group changes its effect on the emission energy from blue- to red-shifting. Furthermore, the combination of these opposite effects and resonance stabilization of the phenolate−keto form causes switching of the order of maximum emission wavelengths of the three species involved in the keto−enol−enolate equilibrium from enol ≪ keto < enolate in absence of 6′-OH to keto < enol ≪ enolate with 6′-OH, to enol < enolate < keto with 6′-O^-. If only the keto−enol−enolate equilibrium is considered, solvents of medium polarity are the most effective in decreasing the excited-state energy. Polar or very polar environments also stimulate shift of the ground-state equilibrium toward the enol form. Under such circumstances, the enol group can be partly or completely deprotonated in the ground state or from the excited state: a polar environment facilitates the ionization, while a less polar environment requires the presence of a stronger base. In the absence of bases, the ground-state keto form exists only in solvents of very weak to medium polarity, but with stronger bases, it can also exist in a nonpolar or very weakly polar environment, usually together with the enolate anion. The phenol−enolate form of oxyluciferin, a species that could not be experimentally detected prior to this study, was identified as a yellow-emitting species.

1. Introduction

The biochemical production of excited states from ground-state reactants, bioluminescence, is an extraordinary natural phenomenon. Fascination with the biochemical origin of its light emission, as well as with its astonishing visual impact, has inspired a vast amount of experimental and model studies. Recently, the mechanistic significance notwithstanding, bioluminescent reactions have become an important platform in the search for alternative sources of light and are now an indispensable tool for bioanalytical applications. The most studied bioluminescent reaction systems currently are those underlying the bioluminescence of jellyfish (notably, the green fluorescence protein)[1−12] and beetles, including fireflies.[13−19] If the efficacy based on fluorescence yield is considered, from all bioluminescent reactions where the emitter exists as a chemically unbound species within the protein matrix, the reaction utilized by the fireflies seems to offer the best promise for that purpose.[20] In fact, the requirement of this reaction for energy-rich species (ATP) and its high fluorescence yield[20] have been already utilized for bioanalytical targets, namely,

(1) Shimomura, O. *Bioluminescence: Chemical Principles and Applications*; World Scientific: Singapore, 2008; pp 151−153.
(2) Solntsev, K. M.; Poizat, O.; Dong, J.; Rehault, J.; Lou, Y.; Burda, C.; Tolbert, L. M. *J. Phys. Chem. B* **2008**, *112*, 2700–2711.
(3) Dong, J.; Abulwerdi, F.; Baldridge, A.; Kowalik, J.; Solntsev, K. M.; Tolbert, L. M. *J. Am. Chem. Soc.* **2008**, *130*, 14096–14098.
(4) Vengris, M.; van Stokkum, I. H. M.; He, X.; Bell, A. F.; Tonge, P. J.; van Grondelle, R.; Larsen, D. S. *J. Phys. Chem. A* **2004**, *108*, 4587–4598.
(5) Chattoraj, M.; King, B. A.; Bublitz, G. U.; Boxer, S. G. *Proc. Natl. Acad. Sci. U.S.A.* **1996**, *93*, 8362–8367.
(6) Leiderman, P.; Ben-Ziv, M.; Genosar, L.; Huppert, D.; Solntsev, K. M.; Tolbert, L. M. *J. Phys. Chem. B* **2004**, *108*, 8043–8053.
(7) Meech, S. R. *Chem. Soc. Rev.* **2009**, *38*, 2922–2934.
(8) van Thor, J. J. *Chem. Soc. Rev.* **2009**, *38*, 2935–2950.
(9) Fang, C.; Frontiera, R. R.; Tran, R.; Mathies, R. A. *Nature* **2009**, *462*, 200–204.
(10) Forbes, M. W.; Jockusch, R. A. *J. Am. Chem. Soc.* **2009**, *131*, 17038–17039.
(11) Leiderman, P.; Huppert, D.; Remington, S. J.; Tolbert, L. M.; Solntsev, K. M. *Chem. Phys. Lett.* **2008**, *455*, 303–306.
(12) Dong, J.; Solntsev, K. M.; Tolbert, L. M. *J. Am. Chem. Soc.* **2009**, *131*, 662–670.
(13) Shimomura, O. *Bioluminescence: Chemical Principles and Applications*; World Scientific: Singapore, 2008; pp 3−22.
(14) Fraga, H. *Photochem. Photobiol. Sci.* **2008**, *7*, 146–158.
(15) Ugarova, N. N. *Photochem. Photobiol. Sci.* **2008**, *7*, 218–227.
(16) Viviani, V. R.; Arnoldi, F. G. C.; Neto, A. J. S.; Oehlmeyer, T. L.; Bechara, E. J. H.; Ohmiya, Y. *Photochem. Photobiol. Sci.* **2008**, *7*, 159–169.
(17) Ugarova, N. N. *J. Biolumin. Chemilumin.* **1989**, *4*, 406–418.
(18) Wood, K. V.; Lam, Y. A.; McElroy, W. D. *J. Biolumin. Chemilumin.* **1989**, *4*, 289–301.
(19) Ugarova, N. N.; Brovko, L. Y. *Luminescence* **2002**, *17*, 321–330.
(20) Ando, Y.; Niwa, K.; Yamada, N.; Enomoto, T.; Irie, T.; Kubota, H.; Ohmiya, Y.; Akiyama, H. *Nat. Photonics* **2007**, *2*, 44–47.

10.1021/ja102885g

Scheme 1. The Proposed Reaction Mechanism of Firefly Bioluminescence

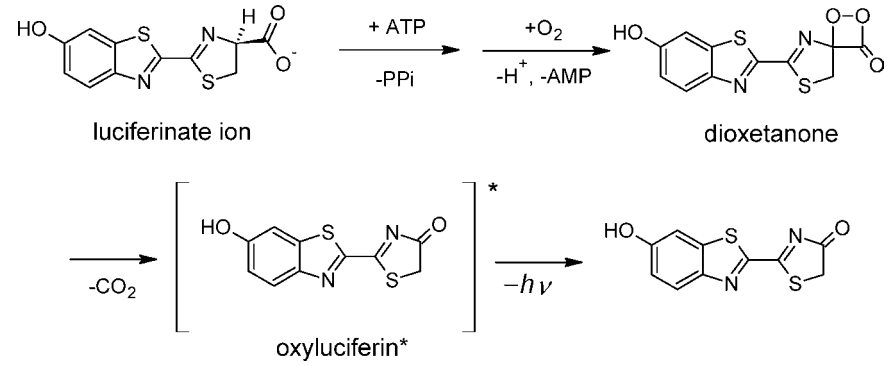

Scheme 2. Chemical Equilibria of Oxyluciferin ($OxyLH_2$, Top) and of 6′-Dehydroxyoxyluciferin (DHOxyLH, Bottom)[a]

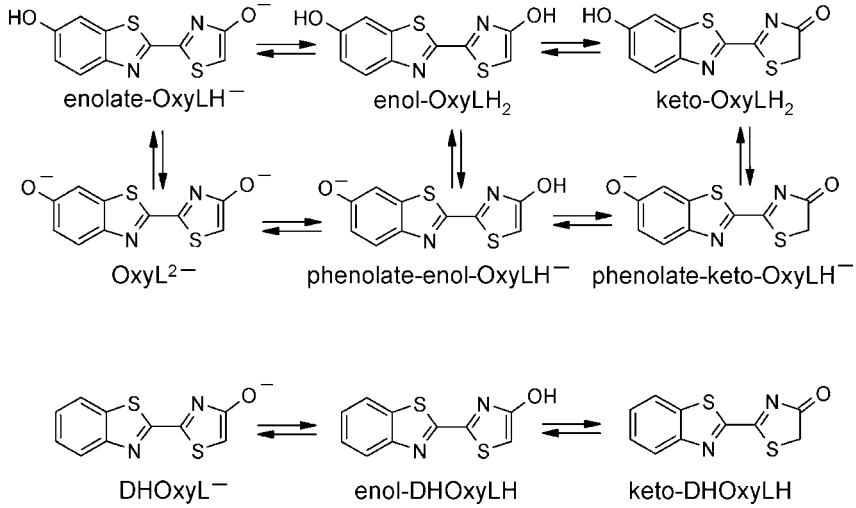

[a] Note that phenolate−keto-$OxyLH^-$ can exist as resonance equilibrium of two limiting structures, with the negative charge at either oxygen atom.

in microbiological analysis,[21,22] in the expression and regulation of genes,[23−26] and in bioluminescence imaging.[27−29] Very recently, bioluminescent probes based on firefly luciferin, which were caged with photoactivatable groups, were successfully applied to real-time *in vivo* monitoring of cell dynamics.[30]

The firefly luciferases are members of a family of click beetle and railroad worm luciferases[16,19] that catalyze a multistep oxidation of the substrate, D(−)-luciferin (LH_2), to an excited-state product, oxyluciferin ($OxyLH_2$), whereupon CO_2 and AMP also appear as products (Scheme 1). Although the spectroscopy of the precursor (LH_2) has been well studied,[31−34] the instability of the emitter ($OxyLH_2$) in basic model solutions has allowed limited insight into its spectroscopy.[35−37] The majority of information has been obtained from substituted model molecules,[37−40] and in fact, it was only recently that we succeeded in determining its crystal structure and were able to more closely examine its absorption and emission spectra.[41] However, the solution chemistry of $OxyLH_2$ turned out to be complex because the molecule can exist as a triple equilibrium of six chemical forms (Scheme 2). In solution, these forms cover a large part (442−626 nm) of the emission spectrum of the natural bioluminescence (530−640 nm). Both $OxyLH_2$ and its precursor have been a subject of extensive theoretical

(21) Griffiths, M. W. *Food Technol.* **1996**, *50*, 62–63.
(22) Contag, C. H. *Mol. Microbiol.* **1995**, *18*, 593–603.
(23) Kricka, L. *Anal. Chem.* **1995**, *67*, 499–502.
(24) Price, R. L.; Squirrell, D. J.; Murphy, M. J. *J. Clin. Ligand Assay* **1998**, *21*, 349–357.
(25) Kricka, L. *Methods Enzymol.* **2000**, *305*, 333–345.
(26) Ohkuma, H.; Abe, K.; Kosaka, Y.; Maeda, M. *Luminescence* **2000**, *15*, 21–27.
(27) Greer, L. F.; Szalay, A. A. *Luminescence* **2002**, *17*, 43–74.
(28) Shinde, R.; Perkins, J.; Contag, C. H. *Biochemistry* **2006**, *45*, 11103–11112.
(29) Contag, C. H.; Bachmann, M. H. *Annu. Rev. Biomed. Eng.* **2002**, *4*, 235–260.
(30) Shao, Q.; Jiang, T.; Ren, G.; Cheng, Z.; Xing, B. *Chem. Commun.* **2009**, 4028–4030.
(31) Wada, N.; Shibata, R. *J. Phys. Soc. Jpn.* **1997**, *66*, 3312–3313.
(32) Wada, N.; Mitsuta, K.; Kohno, M.; Suzuki, N. *J. Phys. Soc. Jpn.* **1989**, *58*, 3501–3504.
(33) Brovko, L. Y.; Cherednikova, E. Y.; Chikishev, A. Y.; Chudinova, E. A. *Moscow Univ. Trans. Phys. Astron. Ser.* **1998**, *3*, 26–29.
(34) Morton, R. A.; Hopkins, T. A.; Selinger, H. H. *Biochemistry* **1969**, *8*, 1598–1607.
(35) Gandelman, O. A.; Brovko, L. Y.; Ugarova, N. N.; Chikishev, A. Y.; Shkurimov, A. P. *J. Photochem. Photobiol.* **1993**, *B19*, 187–191.
(36) Gandelman, O. A.; Brovko, L. Yu.; Chikishev, A. Yu.; Shurinov, A. P.; Ugarova, N. N. *J. Photochem. Photobiol. B.: Biol* **1994**, *22*, 203–209.
(37) White, E. H.; Roswell, D. F. *Photochem. Photobiol.* **1991**, *53*, 131–136.
(38) Hirano, T.; Hasumi, Y.; Ohtsuka, K.; Maki, S.; Niwa, H.; Yamaji, M.; Hashizume, D. *J. Am. Chem. Soc.* **2009**, *131*, 2385–2396.
(39) Leont'eva, O. V.; Vlasova, T. N.; Ugarova, N. N. *Biochemistry (Moscow)* **2006**, *71*, 51–55.
(40) Vlasova, T. N.; Leontieva, O. V.; Ugarova, N. N. *Biochemistry (Moscow)* **2006**, *71*, 555–559.
(41) Naumov, P.; Ozawa, Y.; Ohkubo, K.; Fukuzumi, S. *J. Am. Chem. Soc.* **2009**, *131*, 11590–11605.

Chart 1. Structures of D(−)-Luciferin (LH_2), Oxyluciferin ($OxyLH_2$), 6′-Dehydroxyoxyluciferin (DHOxyLH), 5-Methyloxyluciferin ($MOxyLH_2$), 5,5-Dimethyloxyluciferin (DMOxyLH), 6′-Methoxy-5,5-dimethyloxyluciferin (MDMOxyLH), 4-Dehydroxy-5,5-dimethyloxyluciferin (DHDMOxyLH), and D(−)-5,5-Dimethylluciferin ($DMLH_2$)

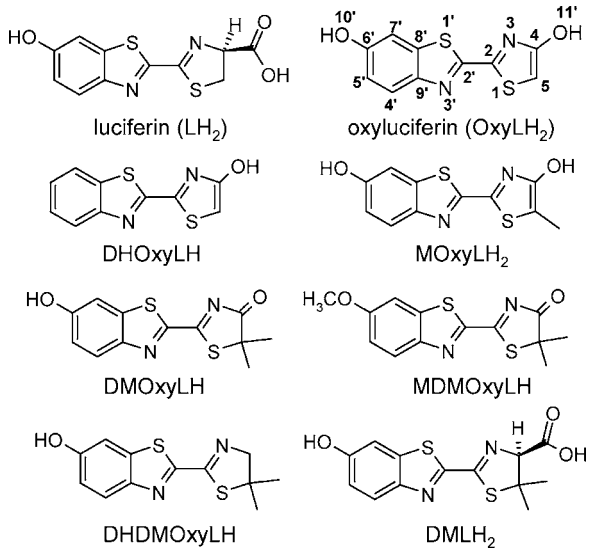

studies.[38,41−50] Experimentally, the phenol−phenolate equilibrium of $OxyLH_2$ was studied recently by Hirano et al.[38] on its dimethyl derivative, DMOxyLH (Chart 1), which is constrained by the 5,5-dimethyl substitution to the keto form. In the study, which was motivated by earlier observations[51,52] that the keto form of $OxyLH_2$ can produce red light in addition to yellow-green light, it was demonstrated that the emission color can be tuned within a wide spectral range (541−640 nm) solely by varying the solvent polarity and the nature of interaction between the phenolate ion and the countercation.

To date, the spectroscopic consequences of the keto−enol equilibrium and the enol deprotonation of $OxyLH_2$ and, especially, the effects of the environment on the double equilibrium of the 4-hydroxythiazole moiety have not been investigated. According to the mechanism described in Scheme 1, the bioluminescence emitter is created in its keto form, which emits light from a chemically produced excited state that decays on a nanosecond time scale.[35,41] The lifetime of the first excited state, therefore, is longer than or comparable to the time scales expected for intramolecular proton transfer (∼100 fs) or proton transfer to the solvent (<10 ns), so (partial) enolization and deprotonation from the excited state cannot be excluded. It should be noted, however, that the results obtained on model emitter molecules, such as the one studied here, where all reactions in Scheme 2 are in principle possible, do not necessarily apply in their entirety to the bioluminescence reaction, where the product is obtained as the excited keto form and, thus, only some of these emitters could be created.

In this work, we turned our attention toward the other two fundamental reactions of the multifunctional oxyluciferin platform, namely, the structural and spectroscopic effects of the enol−keto tautomerism and of the deprotonation of the enol functionality. More specifically, we focused on the model emitter DHOxyLH (Chart 1), which is devoid of the 6′-OH group. Thus, an assessment of the electronic and environmental effects on the enol−keto and enol−enolate equilibria of oxyluciferin can be conveniently accomplished. The choice of DHOxyLH as a model for the real emitter $OxyLH_2$ was also based on several additional considerations. First, although as many as six mechanisms have been proposed for the color tuning (from green to red) of the firefly bioluminescence color,[19,35,38,51−56] the consensus about the origin of this extraordinary phenomenon has not been reached yet. Being devoid of the 6′-OH group, with DHOxyLH, only two of the proposed mechanisms are possible, one of which has been already discredited[42,44,48] on theoretical grounds. Second, we recently observed[41] that the protonation state of the 6′-OH group (phenol versus phenolate) is critical to the emission energies determined by the keto−enol−enolate equilibrium. In particular, the 6′-deprotonation triggers switching of the relative order in the λ_{em}^{max} keto < enol < enolate of the phenol forms of $OxyLH_2$ to enol < enolate < keto of the phenolate forms.[57] The different emission energies of the phenolate ion and the neutral molecule necessitate a model in which the effects of the keto−enol and enol−enolate equilibria on the emission energy can be conveniently isolated from those caused by the phenol−phenolate equilibrium. Third, the polarity of the environment induces opposite effects on the Stokes shifts of the neutral molecule and the phenolate ion;[41] while for the phenol form less polar solvents cause larger Stokes shifts relative to the more polar ones, just the opposite is true for the phenolate form. Therefore, a molecule that is devoid of the 6′-OH group is needed if the environment effects on the chemical equilibrium of the 4-hydroxythiazole fragment are to be assessed. Fourth, because of the notably higher acidity[41] of the phenol group ($pK_a = 7.44$) relative to the enol group ($pK_a = 8.14$), from the six possible forms of $OxyLH_2$, the phenol−enolate form (enolate-$OxyLH^-$ in Scheme 2) has remained the most poorly characterized species. For the first excited state of this yet undetected

(42) Navizet, I.; Liu, Y.-J.; Ferré, N.; Xiao, H.-Y.; Fang, W.-H.; Lindh, R. *J. Am. Chem. Soc.* **2010**, *132*, 706–712.
(43) Chung, L. W.; Hayashi, S.; Lundberg, M.; Nakatsu, T.; Kato, H.; Morokuma, K. *J. Am. Chem. Soc.* **2008**, *130*, 12880–12881.
(44) Nakatani, N.; Hasegawa, J.; Nakatsuji, H. *J. Am. Chem. Soc.* **2007**, *129*, 8756–8757.
(45) Dahlke, E. E.; Cramer, C. J. *J. Phys. Org. Chem.* **2003**, *16*, 336–347.
(46) Li, Z.; Ren, A.; Guo, J.; Yang, T.; Goddard, J. D.; Feng, J. *J. Phys. Chem. A* **2008**, *112*, 9796–9800.
(47) Ren, A.; Guo, J.; Feng, J.; Zou, L.; Li, Z.; Goddard, J. D. *Chin. J. Chem.* **2008**, *26*, 55–64.
(48) Yang, T.; Goddard, J. D. *J. Phys. Chem. A* **2007**, *111*, 4489–4497.
(49) Tagami, A.; Ishibashi, N.; Kato, D.; Taguchi, N.; Mochizuki, Y.; Watanabe, H.; Ito, M.; Tanaka, S. *Chem. Phys. Lett.* **2009**, *472*, 118–123.
(50) Liu, Y.-J.; De Vico, L.; Lindh, R. *J. Photochem. Photobiol. A* **2008**, *194*, 261–267.
(51) Branchini, B. R.; Murtiashaw, M. H.; Magyar, R. A.; Portier, N. C.; Ruggiero, M. C.; Stroh, J. G. *J. Am. Chem. Soc.* **2002**, *124*, 2112–2113.
(52) Branchini, B. R.; Southworth, T. L.; Murtiashaw, M. H.; Magyar, R. A.; Gonzalez, S. A.; Ruggiero, M. C.; Stroh, J. G. *Biochemistry* **2004**, *43*, 7255–7262.
(53) Nakatsu, T.; Ichiyama, S.; Hiratake, J.; Saldanha, A.; Kobashi, N.; Sakata, K.; Kato, H. *Nature* **2006**, *440*, 372–376.
(54) White, E. H.; Rapaport, E.; Selinger, H. H.; Hopkins, T. A. *Bioorg. Chem.* **1971**, *1*, 92–122.
(55) White, E. H.; Rapaport, E.; Hopkins, T. A.; Selinger, H. H. *J. Am. Chem. Soc.* **1969**, *91*, 2178–2180.
(56) McCapra, F.; Gilfoyle, D. J.; Young, D. W.; Church, N. J.; Spencer, P. In *Bioluminescence and Chemiluminescence. Fundamentals and Applied Aspects*; Campbell, A. K., Kricka, L. J., Stanley, P. E., Eds.; John Wiley & Sons: Chichester, U.K., 1994; p 387.
(57) Keto−phenol (442 nm in MeOH, blue) < enol−phenol (463 nm in MeOH, 448 nm in DMSO, blue) < enolate−phenol (theoretical value[44] 580 nm, yellow-orange); enol−phenolate (574 nm in DMSO, yellow-green) < enolate−phenolate (590 nm in DMSO, orange) < keto−phenolate (617 nm in DMSO, red).

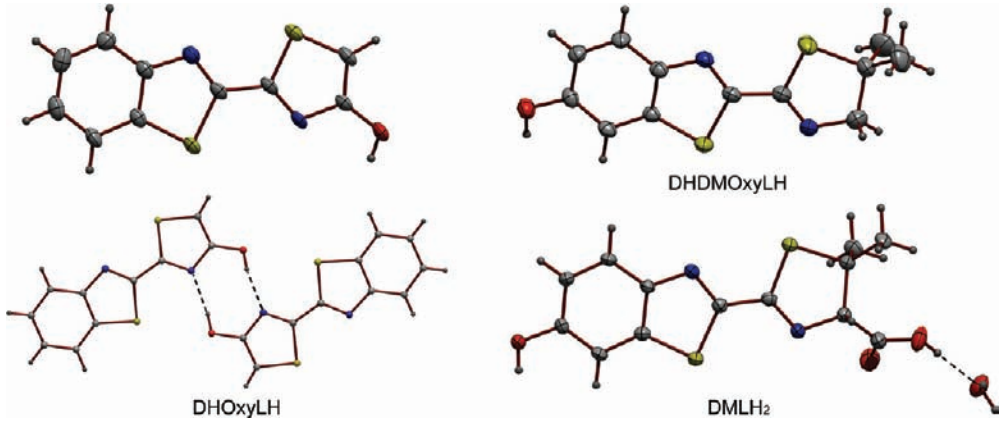

Figure 1. Plots of the molecular structures of the derivatives of oxyluciferin and luciferin determined in this study. The ORTEPs are drawn at 30% probability level.

ion, which in solution might exist only as a minor component in complex mixtures with the other species, the theory predicts emission in the yellow region ($\lambda_{em}^{max} \approx 580$ nm).[44] By having the enol as the only ionizable group and thus by excluding the phenolic and phenolate species from the mixture, with DHOxyLH we are able to characterize the (dehydroxylated) analogue of enolate-OxyLH$^-$ with DHOxyLH.

Hoping to resolve the above issues, here, we investigate in great detail the environmental effects on the steady-state UV−visible and fluorescence spectra of DHOxyLH and its anion (DHOxyL$^-$) obtained in presence of organic bases of different basicity. We also report the crystal structure of the parent molecule, DHOxyLH, and we provide improved structural data on D(−)-LH$_2$, which was first reported in the 1970s.[58−60] Aimed at probing the substituent effects on the structures of OxyLH$_2$ and LH$_2$ and, particularly, the changes that occur in their geometry during the natural bioluminescence, we also report the structures of two new derivatives, namely, 4-dehydroxy-5,5-dimethyloxyluciferin (DHDMOxyLH) and D(−)-5,5-dimethylluciferin (DMLH$_2$) in Chart 1. The precise structural parameters of precursors and analogues of OxyLH$_2$ are of relevance not only to substantiate experimentally the ongoing protein crystallographic analyses of complexed luciferases but also to assess the structural predictions related to the firefly bioluminescence, given the plethora of recent theoretical studies that have been incapable of testing the optimization performance of different models against experimental data.[38,41−50] This study showed that similar to other oxyluciferins, in the solid state, DHOxyLH exists as the enol tautomer, which is paired as hydrogen-bonded dimers. The spectral comparison of DHOxyLH with the other substituted oxyluciferins confirmed the critical role that the deprotonated 6′-O$^-$ group plays in the energy and spectral width of the firefly bioluminescence.

2. Results and Discussion

2.1. Structures. DHOxyLH was prepared in pure form (see Experimental Section) by the general method for synthesis of substituted oxyluciferins of Suzuki and Goto.[61] However, contrary to the original report,[61] according to which the compound was obtained as the keto tautomer, the absence of the carbonyl stretching band in the IR spectrum of our as-synthesized solid product (Figure S1 in the Supporting Information) confirmed that the enol tautomer actually has been obtained. The crystallization of the product proved to be an extraordinarily difficult task, and the result could be improved neither by the use of different solvents nor by exclusion of light or oxygen. Only a couple of times we succeeded in obtaining, at room temperature (RT), a small amount of very tiny (<200 μm) clustered orange crystals by slowly evaporating methanol solution of freshly synthesized DHOxyLH above $CaCl_2$ under nitrogen. X-ray diffraction data[62] were collected at RT from several of these specimens, the best diffracting of which was only $165 \times 45 \times 25\ \mu m^3$. The structure is presented in Figure 1, together with those of the other two molecules determined in this study, and the relevant structural parameters are listed in Table 1. The crystal structure of DHOxyLH has a short stacking axis of 3.85 Å and contains a single type of molecules in the unit cell, which appears slightly disordered in the thiazole ring. The intramolecular parameters are normal and similar to those of the other oxyluciferin analogues (Table 1). Contrary to the expectations based on the relative enol−keto energies, which favor the keto form as more stable tautomer, but in accordance with what we observed with OxyLH$_2$ and MOxyLH$_2$,[41] the packing of DHOxyLH displays head-to-tail hydrogen-bonded dimers of the enol form. Therefore, the conclusion that the enol appears as typical tautomeric form can now be generalized over other crystals of oxyluciferin-like molecules that are not constrained to the keto form. Moreover, the bis-enol dimer based on the doubly hydrogen-bonded synthon (O−H···N)$_2$ appears as a persistent pattern in the supramolecular organization of these emitters in the solid state.

Before 2009, the only known experimental structure of a firefly luciferin or oxylucferin-type molecule and, indeed, of any 2−2′-bridged thiazole−benzothiazole moiety, was that of D(−)-LH$_2$ (the neutral form of the precursor of the firefly

(58) Dennis, D.; Stanford, R. H. *Acta Crystallogr., Sect. B* **1973**, *29*, 1053–1058.
(59) Blank, G. E.; Pletcher, J.; Sax, M. *Acta Crystallogr., Sect. B* **1974**, *30*, 2525–2529.
(60) Blank, G. E.; Pletcher, J.; Sax, M. *Biochem. Biophys. Res. Commun.* **1971**, *42*, 583–588.
(61) Suzuki, N.; Goto, T. *Agric. Biol. Chem.* **1972**, *36*, 2213–2221.
(62) Basic crystallographic data. DHOxyLH: $C_{10}H_6N_2OS_2$, $M_r = 234.29$, monoclinic, $P2_1/c$, $Z = 4$, $a = 18.193(4)$ Å, $b = 3.8471(8)$ Å, $c = 14.112(3)$ Å, $\beta = 91.958(14)°$, $V = 987.2(4)$ Å^3, $R_1 = 6.47\%$. DHDMOxyLH: $C_{12}H_{12}N_2OS_2$, $M_r = 264.36$, orthorhombic, *Pbca*, $Z = 8$, $a = 11.3882(3)$ Å, $b = 10.7673(4)$ Å, $c = 20.4740(8)$ Å, $V = 2510.53(15)$ Å^3, $R_1 = 4.47\%$. D(−)-LH$_2$: $C_{11}H_8N_2O_3S_2$, $M_r = 280.31$, orthorhombic, $P2_12_12_1$, $Z = 4$, $a = 5.3039(2)$ Å, $b = 9.4806(5)$ Å, $c = 23.0485(11)$ Å, $V = 1158.97(9)$ Å^3, $R_1 = 3.81\%$. D(−)-DMLH$_2$: $C_{13}H_{14}N_2O_4S_2 \cdot H_2O$, $M_r = 326.38$, orthorhombic, $P2_12_12_1$, $Z = 4$, $a = 6.0196(7)$ Å, $b = 10.3193(12)$ Å, $c = 23.441(3)$ Å, $V = 1456.1(3)$ Å^3, $R_1 = 2.54\%$. One of the water protons is disordered; the disorder was modeled with two positions of equal occupancy.

Table 1. Selected Experimental Molecular Structural Parameters of Oxyluciferin, D(−)-Luciferin, and Their Derivatives

	compound[b]								
parameter[a]	$OxyLH_2$	DHOxyLH	$MOxyLH_2$	DMOxyLH	MDMOxyLH[c]	MDMOxyLH[c]	DHDMOxyLH	LH_2	$DMLH_2$[d]
2−2′	1.443	1.456	1.447	1.450	1.451	1.451	1.449	1.468	1.457
2−3	1.328	1.311	1.314	1.306	1.299	1.299	1.275	1.278	1.280
3−4	1.361	1.372	1.361	1.408	1.412	1.408	1.459	1.476	1.461
4−5	1.340	1.349	1.358	1.534	1.543	1.548	1.526	1.518	1.547
5−1	1.587	1.693	1.719	1.834	1.832	1.819	1.843	1.816	1.847
1−2	1.705	1.704	1.707	1.735	1.748	1.745	1.749	1.750	1.744
2′−3′	1.290	1.291	1.302	1.307	1.302	1.305	1.294	1.296	1.295
3′−9′	1.408	1.388	1.391	1.377	1.383	1.375	1.380	1.387	1.375
9′−4′	1.424	1.382	1.392	1.408	1.408	1.406	1.388	1.392	1.392
4′−5′	1.367	1.378	1.369	1.376	1.366	1.373	1.369	1.381	1.363
5′−6′	1.399	1.380	1.409	1.413	1.414	1.409	1.393	1.398	1.395
6′−7′	1.371	1.355	1.374	1.390	1.390	1.394	1.384	1.379	1.375
7′−8′	1.388	1.388	1.393	1.392	1.395	1.399	1.384	1.396	1.397
8′−1′	1.733	1.734	1.727	1.729	1.731	1.734	1.725	1.729	1.734
1′−2′	1.732	1.738	1.740	1.750	1.754	1.749	1.751	1.741	1.737
8′−9′	1.381	1.399	1.403	1.415	1.410	1.413	1.402	1.398	1.403
4−11′	1.338	1.344	1.341	1.211	1.210	1.216		1.530	1.509
6′−10′	1.358		1.361	1.363	1.365	1.363	1.358	1.365	1.360
1−2−3	114.6	114.7	114.4	119.2	119.7	120.3	117.8	119.6	118.6
2−3−4	109.5	109.7	110.1	110.8	110.8	110.1	111.3	110.5	110.1
3−4−5	115.5	115.8	116.9	114.9	115.1	115.1	111.1	109.2	110.4
4−5−1	111.2	109.8	108.3	104.0	104.4	104.6	102.4	105.8	101.0
5−1−2	89.2	90.0	90.3	90.2	90.1	89.9	90.0	88.2	89.5
1′−2′−3′	116.7	116.8	116.1	116.7	116.5	116.7	116.3	116.0	116.3
2′−3′−9′	110.0	110.0	110.4	109.8	110.2	110.1	110.3	110.7	110.5
2′−1′−8′	88.6	88.7	89.1	88.5	88.5	88.4	88.5	88.9	88.9
1′−2′−2−3	−1.1	5.1	−2.7	0.1	−2.9	4.1	3.9	−1.7	5.1
3′−2′−2−1	−1.6	5.6	−2.0	−1.2	−1.6	3.2	4.9	−0.8	5.4
3′−2′−2−1′	177.8	179.2	179.5	177.2	−178.7	179.42	−178.5	−178.6	179.1
1−2′−2−3	178.3	178.6	178.8	178.4	180.0	−179.7	−179.5	−179.5	178.8
twist[e]	3.3	5.7	2.7	3.7	2.5	3.7	4.7	2.0	5.5
ω[f]	−1.3	5.3	−2.3	−0.5	−2.2	3.6	4.4	−1.2	5.2
$\chi(2')$[f]	−2.2	−0.8	−0.5	−2.8	+1.3	−0.6	+0.9	+1.9	−0.9
$\chi(2)$[f]	−1.7	−1.4	−1.2	−1.6	0.0	+1.6	+0.5	+2.4	−1.2

[a] Distances are given in ångströms; angles are in degrees. For the atom labels, see $OxyLH_2$ in Chart 1. [b] The acronyms refer to Chart 1. References: $OxyLH_2$,[41] DHOxyLH (this work), $MOxyLH_2$,[41] DMOxyLH,[38] MDMOxyLH,[38] DHDMOxyLH (this work), LH_2 (the structure was redetermined in this work), $DMLH_2$ (this work). [c] The crystal contains molecules of two crystallographic types.[38] [d] The acid exists as monohydrate, $DMLH_2 \cdot H_2O$. [e] In order to bring the luciferins (nonplanar at the thiazole ring) and the oxyluciferins (planar at the thiazole ring) on the same scale, the twist around the 2−2′ bond was defined here as the dihedral angle between the planes 1−2−3 and 1′−2′−3′. Note that this convention is different from that employed by us previously,[41] where the angle was calculated on all atoms of the cyclic skeleton. [f] Definition of the distortion parameters (the atom labels refer to Chart 1): $\omega = {}^1/_2[\tau(1'-2'-2-3) + \tau(3'-2'-2-1)]$; $\chi(2') = [\tau(3'-2'-2-1') \bmod 360°] - 180°$; $\chi(2) = [\tau(1-2'-2-3) \bmod 360°] - 180°$.[63]

bioluminescence), which was independently reported twice about 40 years ago.[58−60] In the course of this study, we have determined the structures of three new molecules based on the $OxyLH_2/LH_2$ platform, and we have also redetermined the structure of D(−)-LH_2 by using modern diffraction methods.[62] Together with the structures of $OxyLH_2$ and $MOxyLH_2$[41] and the two 4,4-dimethyl analogues of $OxyLH_2$ that were reported recently[38] (one of which contains two independent molecules in the structure), these now allow a detailed insight into the geometrical changes that occur in the emitter as a result of the bioluminescence reaction and can also reveal the general preferences regarding the intermolecular interactions of $OxyLH_2$-type fluorophores. Specifically, we compared the geometries (Table 1) of the molecules in Chart 1 to assess the effects of (a) conversion of luciferin into oxyluciferin (D(−)-LH_2 vs $OxyLH_2$), (b) 4-carboxylic group substitution on the luciferin (DHDMOxyLH vs $DMLH_2$), (c) 4-keto substitution in the keto-oxyluciferin (DHDMOxyLH vs DMOxyLH), (d) 5-methyl and 5,5-dimethyl substitution on oxyluciferin ($OxyLH_2$ vs $MOxyLH_2$/DMOxyLH), (e) 5-methyl substitution on luciferin (LH_2 vs $DMLH_2$), and (f) 6′-hydroxy substitution on oxyluciferin (DHOxyLH vs $OxyLH_2$). The largest differences in the bond distances and angles, above the threshold of 0.010 Å and 3°, which illustrate these effects, are shown in Chart 2.

The substitution of the carboxylic group in the thiazole−benzothizole structure has a minor effect on the geometry of the precursor, luciferin, and results in stretching of the C4−C5 bond (+0.021 Å). The increased conjugation by conversion of luciferin into the enol form of oxyluciferin, however, causes strong overall compression of the thiazole ring, mainly at the N3−C4−C5−S1 fragment (−0.115, −0.178, −0.229 Å) and shortens the 2−2′ bridge (−0.025 Å), causing additional distortions in the phenyl ring. The change of hybridization causes opening of the angles at C4 and C5 (+6.3° and +5.4°), which is compensated by compression at the bridging atom C2 (−5.0°). Introduction of the keto group shortens the single bonds N3−C4 (−0.051 Å) and C2−S1 (−0.014 Å), stretches the single bond C2′−N3′ (+0.013 Å), and widens the angle at C4 (+3.8°). Enolization of the keto group causes shortening of the C4−C5 bond from 1.534 Å ($DMOxyLH_2$) to 1.340 Å ($OxyLH_2$). The 5-methyl substitution has a significant effect on the whole molecule, and it is thus expected to affect the electronic structure of the emitter significantly; most importantly, it stretches the adjacent bonds S1−C5 and C5−C4 (+0.132 Å and +0.018 Å). The effect is enhanced with the dimethyl substitution (+0.247 Å and +0.194 Å), which also decreases the angle at C5 (−7.2°).

(63) Radhakrishnan, T. P.; Agranat, I. *Struct. Chem.* **1991**, *2*, 107–115.

Chart 2. The Largest Differences in the Experimental Geometry between Oxyluciferin and Luciferin Molecules Selected To Reflect the Effects of Substitution or That of the Bioluminescence Reaction[a]

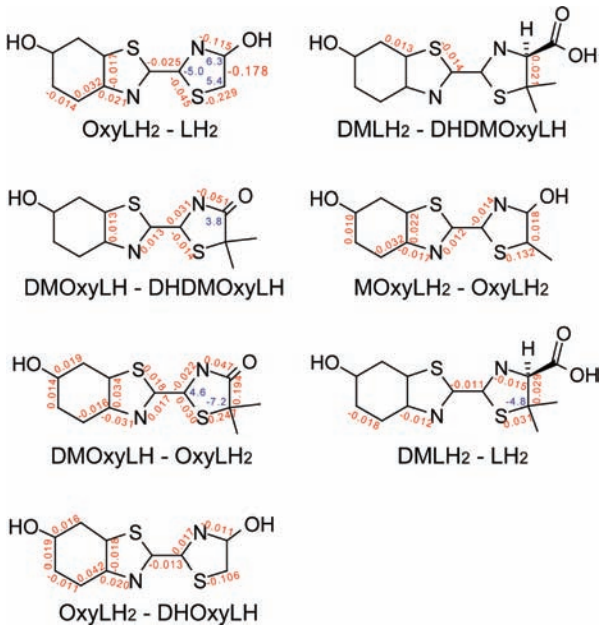

[a] Only differences in bond lengths (red) and angles (blue) larger than 0.010 Å and 3° are shown. The ring double bonds have been omitted for clarity.

A similar but smaller effect was observed for luciferin (+0.031 Å, +0.029 Å, and −4.8°). In contrast, the 6′-OH substitution shortens the S1−C5 bond (−0.106 Å), as it affects (to a lesser degree) the rest of the molecule. All molecules are slightly twisted at the 2−2′ bridge, the twist being largest with DHOxyLH (5.7°) and $DMLH_2$ (5.5°). The pyramidalization[63] at the bridging carbon atoms is small (<2.8°), and except for MDMOxyLH, with the same sign, so that the molecules are almost always slightly bent at the bridge on the same side. The largest pyramidalization (2.8°) was observed with DMOxyLH.

2.2. Spectra. 2.2.1. Steady-State UV−Visible Spectra of DHOxyLH. The presence of an enolizable group at the thiazole ring turns DHOxyLH into a weak monobasic acid. In a series of phosphate-buffered aqueous solutions with varying pH (Figure 2), it showed one isosbestic point, corresponding to the dissociation of the enol group. Under these conditions, the pK_a in water obtained by fitting of the plot of the maximum absorbance was 7.20, which is significantly lower than that of the enol group of $OxyLH_2$ (pK_a = 8.14).[41] The stronger acidity of DHOxyLH may be due to the absence of the additional hydroxyl group, or, alternatively, the previous assignment of the two pK_a values of $OxyLH_2$ may need to be revised. Similar to what has been observed with $OxyLH_2$,[41] the absorption maximum of the conjugate base $DHOxyL^-$ (412 nm) is red-shifted relative to the neutral molecule (361 nm).

The absorbance and emission spectra of DHOxyLH were recorded in 18 solvents of varying polarity.[64] The absorption and emission maxima are listed in Tables 2 and 3, together with the values of the respective concentrations, absorbances, emission intensities, and molar absorption coefficients. For all solvents, the spectra were obtained in the absence of a base (NB) or with a large excess of each of three organic bases: butyl amine (BA, pK_a(H^+−BA;ACN) = 18.3), tributyl amine (TBA, pK_a(H^+-TBA;ACN) = 18.1), and 1,8-diazabicyclo[5.4.0]undec-7-ene (DBU, pK_a(H^+-DBU;ACN) = 24.1).[65,66] These bases were selected because they can provide means for comparison of the solvent effects on the enol(keto) functionality with those on the 6′-OH group, which have been reported previously with DMOxyLH.[38]

The spectra of pure DHOxyLH in the absence of a base are shown in Figure 3 (the individual absorption and emission spectra of DHOxyLH in each solvent are deposited as Figure S2 in the Supporting Information). The absorption maxima of DHOxyLH are relatively uniform and exhibit a single absorption band around 361 nm. The maximum shift of the absorbance is 19 nm, from 348 nm in CH_2Cl_2 to 367 nm in dimethylsulfoxide (DMSO), *m*-xylene, and CCl_4. From the ^{1}H NMR spectrum in DMSO-d_6, it was concluded that this absorption band is due to the lowest excitation of the enol form, enol-DHOxyLH (Figures S3−S5 in the Supporting Information). In fact, the ^{1}H NMR spectra evidenced that in perdeuterated DMSO and methanol at RT, DHOxyLH existed entirely as enol-DHOxyLH; the amount of the anion in methanol-d_4 was insignificant, and no measurable amounts of the keto form could be detected. In DMSO-d_6, the resonance of the enol proton appeared as a singlet peak at 11.11 pm (in methanol-d_4, this peak remained undetectable due to the fast exchange with the solvent). The thiazole proton gave a singlet at 6.46 ppm ($CDCl_3$), 6.49 ppm (CD_3CN), 6.60 ppm (DMSO-d_6), or 6.42 ppm (methanol-d_4). In $CDCl_3$ and CD_3CN, however, a new singlet peak from the protons of the methylene group (2H) appeared at 4.11 and 4.14 ppm, respectively (Figure S5 in the Supporting Information). The aromatic peaks were doubled, and the peaks from the second component were shifted to higher field. This observation clearly evidenced that in these two solvents, the neutral enol form of DHOxyLH existed in equilibrium with the neutral keto form, keto-DHOxyLH, which was confirmed by the intensity ratio of the methylene and the phenylene protons. At RT, the population ratios keto/enol in $CDCl_3$ and CD_3CN calculated from the averaged peak intensities were 21.3%:78.7% and 15.9%:84.1%, respectively.

Similar to the absorption maximum of enol-DHOxyLH, its main emission band around 438 nm, which corresponds to the deexcitation of (enol-DHOxyLH)*, was shifted by nonaqueous solvents 19 nm, between 432 nm in ethyl acetate and 451 nm in DMSO (Figure 3). In water, however, the emission spectrum consisted of a single, strong emission band at 541 nm from the enolate ion ($DHOXyL^-$)*, as evidenced by the identical positions of this band with that obtained by deexcitation of the ion that had been produced by addition of bases and subsequently excited at 413 or 415 nm (see the discussion below). The large Stokes shift of 9217 cm^{-1} observed for the fluorophore in water, which was nearly 1.9 times larger than the average for the other solvents, showed that in water, the most polar solvent, the molecule was completely deprotonated following the excitation. Similar, albeit less complete, excited-state deprotonation of the enol form, (enol-DHOxyLH)* → (enol-$DHOxyL^-$)* + H^+, manifested as a weak band at >500 nm in

(64) Because the solubility of the compound in hexane was much lower than that in the other cases, in this particular case we were able to record spectra only from very diluted solutions.

(65) Kolthoff, I. M.; Chantooni, M. K.; Bhowmik, S. *J. Am. Chem. Soc.* **1968**, *90*, 23–28.
(66) Galezowski, W.; Jarczewski, A.; Stanczyk, M.; Brzezisnki, B.; Bartl, F.; Zundel, G. *J. Chem. Soc., Faraday Trans.* **1997**, *93*, 2515–2518.

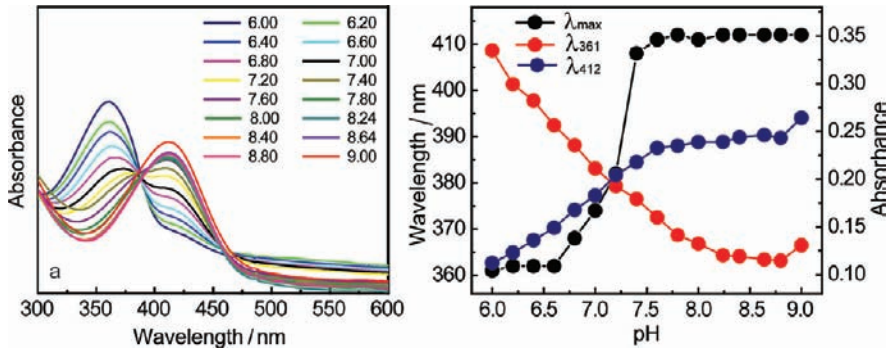

Figure 2. Dependence of the absorption spectrum of DHOxyLH (left) in phosphate-buffered aqueous solution (inset, pH of the solutions) and pH-profile (right) of the wavelength at maximum absorbance (left ordinate) and the absolute absorbance at 361 nm (λ_{361}) and at 412 nm (λ_{412}) (right ordinate).

Table 2. Absorption Spectra of DHOxyLH in Various Solvents

				NB[a]			BA		TBA		DBU	
	solvent	E_T (N)	c (μM·L^{-1})	λ_{max} (nm)	abs	$\varepsilon_{max}/10^4$ (L·mol^{-1} cm^{-1})	λ_{max} (nm)	abs	λ_{max} (nm)	abs	λ_{max} (nm)	abs
1	water	1.000	18.18	361	0.3942	2.17	413	0.3418	413	0.3505	415	0.3389
2	methanol	0.762	18.18	361	0.4456	2.45	414	0.3419	414	0.3189	414	0.3433
3	ethanol	0.654	18.18	362	0.6056	3.33	423	0.4332	364	0.4371	423	0.4712
									420[b]	0.1900[b]		
4	1-butanol	0.586	18.33	363	0.5189	2.83	370	0.2720	364	0.4869	426	0.2125
							425[b]	0.2125[b]	428[b]	0.0815[b]		
5	2-propanol	0.546	18.33	361	0.4123	2.25	373	0.1886	362	0.3942	432	0.3173
							430[b]	0.1839[b]				
6	acetonitrile	0.460	18.18	355	0.5020	2.76	359	0.3001	356	0.4041	454	0.3284
				461[b]	0.0466[b]	0.26[b]	447[b]	0.0481[b]	432[b]	0.0931[b]		
7	dimethylsulfoxide	0.444	18.18	367	0.4298	2.36	368	0.3272	367	0.4214	496	0.2925
							485[b]	0.0563[b]				
8	dimethylformamide	0.386	18.33	365	0.5410	2.95	366	0.3921	365	0.5237	472	0.3152
				460[b]	0.0329[b]	0.18[b]	463[b]	0.0715[b]	459[b]	0.0469[b]		
9	acetone	0.355	18.18	358	0.7128	3.92	361	0.4693	359	0.6779	450	0.4003
10	1,2-dichloroethane	0.327	18.33	359	0.5582	3.05	364	0.4567	364	0.4318	442	0.3872
11	dichloromethane	0.309	18.18	348	0.4695	2.58	362	0.3833	363	0.3356	441	0.3556
							441[b]	0.0925[b]	429[b]	0.1060[b]		
12	chloroform	0.259	18.18	356	0.5149	2.83	356	0.3513	363	0.3356	430	0.3717
									431[b]	0.1025[b]		
13	ethyl acetate	0.228	18.18	359	0.5769	3.17	363	0.5348	359	0.5451	368	0.4906
14	benzene	0.111	18.33	366	0.6848	3.74	368	0.6224	366	0.6580	391	0.3604
											445[b]	0.2731[b]
15	toluene	0.099	18.33	366	0.5993	3.27	369	0.5665	368	0.5788	388	0.3626
											444[b]	0.2080[b]
16	*m*-xylene		18.33	367	0.6611	3.61	369	0.6457	366	0.6342	386	0.4110
											447[b]	0.1858[b]
17	carbon tetrachloride	0.052	18.33	367	0.3794	2.07	367	0.3561	368	0.3719	384	0.2341
											445[b]	0.0994[b]
18	hexane	0.009	18.33	360	0.0111	0.06	367	0.0369	367	0.0098	459	0.2635

[a] No base added. [b] Shoulder/second peaks.

other polar solvents (for instance, DMSO and water). The partial excited-state deprotonation was particularly apparent in alcohols (methanol, $\lambda^{em}_{max,2} \approx 547$ nm; ethanol, $\lambda^{em}_{max,2} \approx 550$ nm; 2-propanol, $\lambda^{em}_{max,2} \approx 548$ nm; 1-butanol, $\lambda^{em}_{max,2} \approx 550$ nm), DMSO ($\lambda^{em}_{max,2} \approx 585$ nm), and DMF ($\lambda^{em}_{max,2} \approx 583$ nm). This result demonstrated that in polar or medium-polarity environments, the enol group of DHOxyLH can be partially or completely deprotonated from the excited state, resulting in large Stokes shifts and a secondary, weak green-yellow emission (541−585 nm).

2.2.2. UV−Visible Spectra of Deprotonated DHOxyLH. The spectra of DHOxyLH in the 18 solvents recorded in the presence of bases are presented in Figure 4. The spectra recorded after the addition of bases to DHOxyLH in four (aprotic and protic) solvents, which were selected to cover the range of solvent polarities employed in this study, are shown in Figure 5. As can be inspected from there, the ratio of the three forms of DHOxyLH depends on the solvent polarity, as well as on the basicity of the base. The Lippert−Mataga plots[67,68] for DHOxyLH and its deprotonated analogue (Figure 6) deviate strongly from linearity, indicating significant effects of the specific interactions on the excitation and emission energies. As will be detailed in the discussion below, the two groups of outlying points with large Stokes shifts in this plot can be attributed to excited-state keto−enolate isomerization, in accordance with what has been observed previously with $OxyLH_2$[41] and DMOxyLH.[38]

(67) Lippert, E. Z. *Electrochemistry* **1957**, *61*, 962–975.
(68) Mataga, N.; Kaifu, Y.; Koizumi, M. *Bull. Chem. Soc. Jpn.* **1956**, *29*, 465–471.

Table 3. Emission Spectra of DHOxyLH in Various Solvents

				NB[a]			BA			TBA			DBU		
	Solvent	E_T(N)	c (μM·L^{-1})	λ_{exc} (nm)	λ_{max} (nm)	FI	λ_{exc} (nm)	λ_{max} (nm)	FI	λ_{exc} (nm)	λ_{max} (nm)	FI	λ_{exc} (nm)	λ_{max} (nm)	FI
1	water	1.000	1.818	361	541	0.1562	413	544	0.3461	413	542	0.3375	415	543	0.2764
2	methanol	0.762	1.818	361	440	0.0730	415	553	0.1907	413	549	0.0324	415	553	0.1973
					547[b]	0.0361[b]									
3	ethanol	0.654	1.818	361	440	0.2423	429	552	0.2949	365	440	0.1824	423	553	0.3532
					550[b]	0.0430[b]					551[b]	0.0549[b]			
										419[c]	556[c]	0.1108[c]			
4	1-butanol	0.586	1.833	363	441	0.4197	372	443	0.1535	364	440	0.3812	435	554	0.3757
								551[b]	0.0824[b]		550[b]	0.0424[b]			
							430[c]	555[c]	0.2378[c]						
5	2-propanol	0.546	1.833	362	439	0.2624	371	437	0.1292	361	440	0.2356	432	555	0.2468
					548[b]	0.0320[b]		547[b]	0.0438[b]		545[b]	0.0332[b]			
							430[c]	554[c]	0.1184[c]						
6	acetonitrile	0.460	1.818	356	434	0.8826	357	430	0.4113	356	433	0.5419	453	586	0.1248
					586[b]	0.0051[b]		585[b]	0.0265[b]		583[b]	0.0271[b]			
7	dimethylsulfoxide	0.444	1.818	367	451	0.1853	365	448	0.0749	367	450	0.1591	495	592	0.2066
					585[b]	0.0695[b]		586[b]	0.0304[b]		588[b]	0.0598[b]			
							493[c]	595[c]	0.1265[c]						
8	dimethylformamide	0.386	1.833	367	449	0.2115	368	450	0.1761	365	448	0.1861	472	596	0.1005
					583[b]	0.0306[b]		582[b]	0.0286[b]		580[b]	0.0281[b]			
9	acetone	0.355	0.909	359	434	0.5086	361	433	0.3510	359	433	0.4368	452	587	0.0449
10	1,2-dichloroethane	0.327	1.833	360	436	0.6104	364	436	0.1575	365	436	0.1215	443	559	0.0759
								554[b]	0.1207[b]		556[b]	0.0944[b]			
11	dichloromethane	0.309	1.818	349	434	0.3995	362	434	0.1487	360	434	0.1559	445	561	0.2447
								554[b]	0.0890[b]		546[b]	0.0908[b]			
12	chloroform	0.259	1.818	356	433	0.2786	360	434	0.1825	361	555	0.2445	429	556	0.1108
								549[b]	0.0512[b]						
13	ethyl acetate	0.228	1.818	359	432	0.5441	362	435	0.0887	359	431	0.2314	369	434	0.2032
								552[b]	0.0024[b]					555[b]	0.0023[b]
14	benzene	0.111	0.916	366	438	0.7670	364	438	0.1765	365	436	0.2440	390	568	0.0818
								556[b]	0.0697[b]		542[b]	0.0987[b]	446[c]	572[c]	0.0641[c]
15	toluene	0.099	0.916	366	439	0.7105	368	439	0.2399	367	440	0.3730	386	573	0.0930
								557[b]	0.0602[b]		549[b]	0.0784[b]	447[c]	572[c]	0.0556[c]
16	*m*-xylene		0.916	367	435	0.6005	370	433	0.1529	367	435	0.3053	386	577	0.0131
								555[b]	0.0461[b]		544[b]	0.0510[b]	449[c]	580[c]	0.0611[c]
17	carbon tetrachloride	0.052	1.833	367	439	0.6760	368	443	0.2131	370	439	0.3350	385	443	0.1256
														541[b]	0.0446[b]
18	hexane	0.009	1.833	361	439	0.2829	365	437	0.1654	370	439	0.4472	459	563	0.4140

[a] No base added. [b] Shoulder/second peaks. [c] Second excitation.

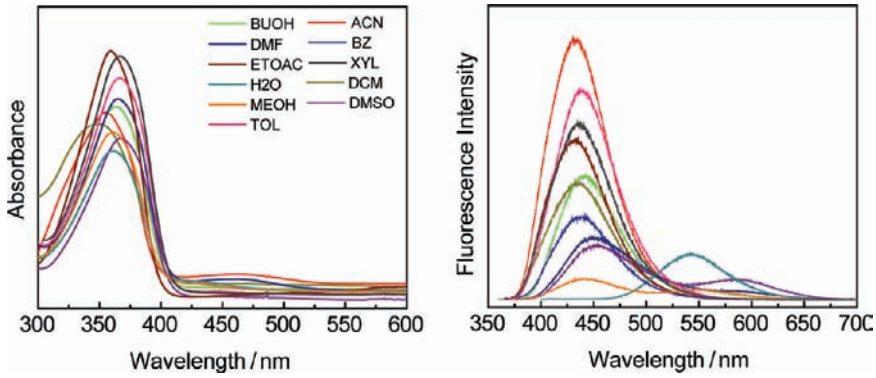

Figure 3. Absorption spectra (left) and fluorescence spectra (right) of DHOxyLH in various solvents (all spectra are deposited as Supporting Information). Solvents (the same color codes apply to both panels): H2O, water; MEOH, methanol; BUOH, 1-butanol; ACN, acetonitrile; DMSO, dimethyl sulfoxide; DMF, dimethylformamide; DCM, dichloromethane; ETOAC, ethyl acetate; BZ, benzene; TOL, toluene; XYL, *m*-xylene. Note that for clarity of presentation, some of the spectra in the common plots were occasionally scaled or offset along the *y*-axis, so that the absolute values of the absorbance/emission are not always directly comparable.

In nearly nonpolar solvents, such as benzene, toluene, or carbon tetrachloride, the addition of either of the two weaker bases (BA and TBA) practically did not affect the chemical state of DHOxyLH (Figure 5a), which existed in these solvents as the pure enol tautomer, enol-DHOxyLH (at higher concentrations, the molecules of this tautomer can probably assemble as hydrogen-bonded homodimers (enol-DHOxyLH)$_2$, similar to those that were observed in the solid state). Correspondingly, the excitation energy (366 nm) was practically identical to that of the pure chromophore in DMSO (367 nm), where the molecule existed as the neutral enol form (NMR). In the presence of BA or TBA in benzene, enol-DHOxyLH did not exhibit notable solvatochromism, and the 366 nm absorption maximum was red-shifted by less than 2 nm. In the presence of the stronger base (DBU), however, the absorption profile changed drastically, and the peak at 366 nm was replaced by

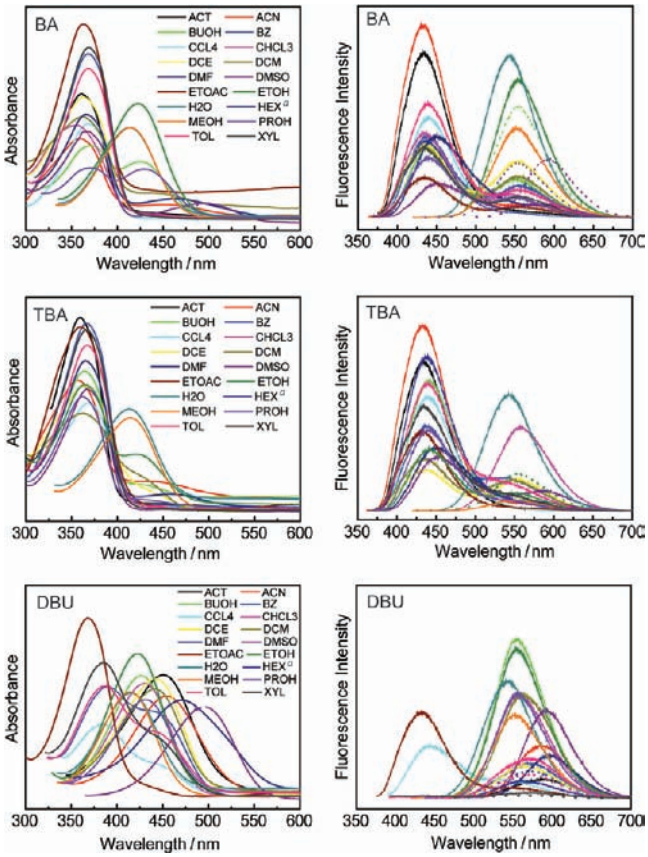

Figure 4. Effects of addition of base on the absorption (left panels) and fluorescence (right panels) spectra of DHOxyLH. Solvents: H2O, water; MEOH, methanol; ETOH, ethanol; BUOH, 1-butanol; PROH, 2-propanol; ACN, acetonitrile; DMSO, dimethyl sulfoxide; DMF, dimethylformamide; ACT, acetone; DCE, 1,2-dichloroethane; DCM, dichloromethane; CHCL3, chloroform; ETOAC, ethyl acetate; BZ, benzene; TOL, toluene; XYL, *m*-xylene; CCL4, carbontetrachloride; HEX, hexane. Bases: BA, butyl amine; TBA, tributyl amine; DBU, 1,8-diazabicyclo[5.4.0]undec-7-ene. Due to much lower solubility of DHOxyLH in hexane, the absorption spectrum is not shown (deposited as Supporting Information). The dotted lines correspond to emission spectra recorded at a second excitation wavelength (Table 3).

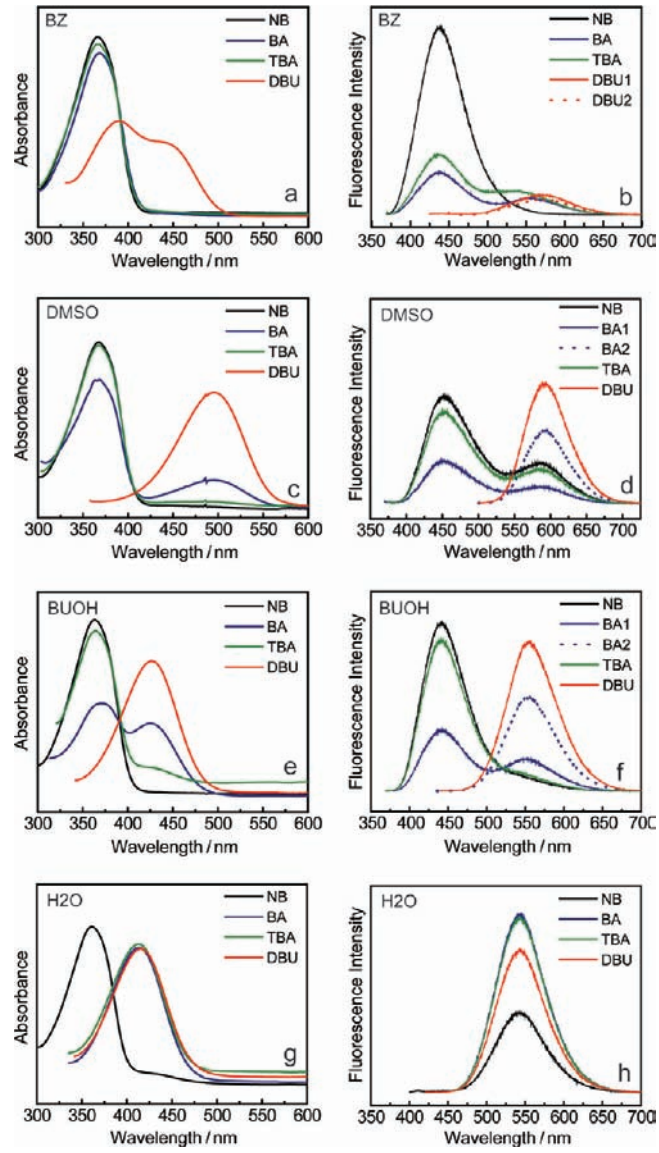

Figure 5. Solvent effects on the absorption (left panels) and fluorescence (right panels) spectra of DHOxyLH in benzene (BZ), dimethyl sulfoxide (DMSO), 1-butanol (BUOH), and water (H2O) in the absence (NB) and in the presence of bases. Bases: BA, butyl amine; TBA, tributyl amine; DBU, 1,8-diazabicyclo[5.4.0]undec-7-ene. The dotted lines correspond to emission spectra recorded at a second excitation wavelength (Table 3).

two overlapped peaks of similar intensity at 391 and 445 nm. This result showed clearly that enol-DHOxyLH was converted into the other two species, keto-DHOxyLH and $DHOxyL^-$. In support of these assumptions, the theoretical calculations on the real firefly emitter, $OxyLH_2$,[44] have predicted lower absorption energy in DMSO (larger red shift) of the phenol−enolate ion (580 nm) relative to the neutral keto form (421 nm), along with the assignment of the peaks at 445 and 391 nm to $DHOxyL^-$ and keto-DHOxyLH, respectively (this assignment was also supported by the spectra recorded from protic solvents, as is explained below). The apparent stabilization of keto-DHOxyLH with DBU in typically nonpolar solvents (benzene, toluene, or carbon tetrachloride) can be rationalized by the unavailability of strong hydrogen proton acceptors from the solvent, which would otherwise stabilize the enol tautomer. Therefore, in nonpolar environments, strong bases induce shift of the double equilibrium keto−enol−enolate from the enol form toward the keto tautomer and the enolate ion.

The emission spectrum in benzene, a typical low-polarity solvent, peaks at 438 nm (Figure 5b). As with the absorption band, this position of the emission from (enol-DHOxyLH)* remained practically unaffected (1−3 nm) by addition of a base, although its intensity was significantly reduced. The insensitivity of the emission energy of (enol-DHOxyLH)* to bases indicated that the respective transition originates from the enol form, a portion of which has remained nondissociated by the base. In presence of bases, however, new red-shifted emission peaks appeared, showing that additional reactions were operative in the excited state. The two weaker bases (TBA and BA) stimulated emission mostly from the excited keto form, (keto-DHOxyLH)*, with overlapped peaks around $\lambda_{em}^{max} \approx 542$ nm (TBA) and $\lambda_{em}^{max} \approx 556$ nm (BA). The red shift of the emission from (keto-DHOxyLH)* relative to (enol-DHOxyLH)* is probably caused by inherent intramolecular factors (lower transition energy), but it might be also affected by intermolecular factors (absence of stabilization by dimerization). However, with a stronger base (DBU), selective excitation of both keto-DHOxyLH ($\lambda_{ex} = 390$ nm) and $DHOxyL^-$ ($\lambda_{ex} = 446$ nm) resulted in emission exclusively from $(DHOxyL^-)$* at $\lambda_{em}^{max} \approx$ 568−572 nm, without any detectable signature of (enol-DHOxyLH)*. This result indicated that the keto species, which

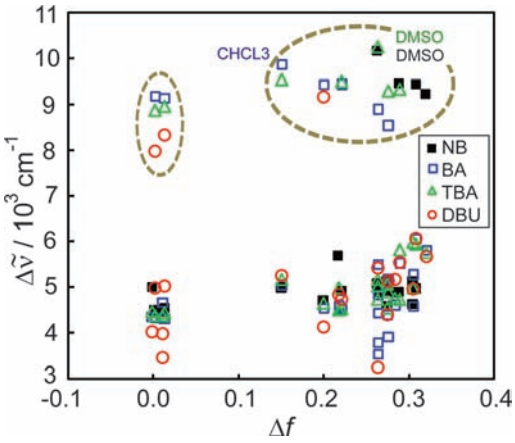

Figure 6. Lippert−Mataga plot for DHOxyLH. Bases: NB, no base added; BA, butyl amine; TBA, tributyl amine; DBU, 1,8-diazabicyclo[5.4.0]undec-7-ene.

existed in equilibrium with the enolate ion, had been *enolized and deprotonated* before deexcitation occurred.

Inspection of the absorption spectra in aprotic solvents of medium polarity showed that under these conditions, DHOxyLH existed as mixtures with varying concentrations of the enol and the enolate (Figure 5c; for other solvents, see Figure S2 in the Supporting Information). For instance, in DMSO in the absence of base or with TBA in DMSO, the molecule existed exclusively as the enol form. Addition of DBU resulted in complete deprotonation, and no ground-state keto form could be detected spectroscopically (Figure 5d). In fact, DMSO presents a special case among the 18 solvents, where in the presence of DBU, the absorption maximum of DHOxyL$^-$ (λ_{abs}^{max} = 496 nm) undergoes the strongest red shift from the respective enol form (λ_{abs}^{max} = 367 nm). Whereas with DBU DHOxyLH is completely ionized even in the ground state and with BA it is partially deprotonated, with TBA it remains neutral (Figure 5c). The anion (DHOxyL$^-$)*, obtained by reaction with DBU and excited from the ground state, emitted in DMSO at λ_{em}^{max} = 592 nm (Figure 5d). Excitation of the enol form in the absence of base or with BA or TBA resulted in partial deprotonation. The ion produced by excited-state dissociation emitted with λ_{em}^{max} = 586 nm (with BA), as did the same species excited from the ground state.

In protic solvents, such as 1-butanol (Figure 5e), we could detect only two species, nearly pure enol-DHOxyLH in the absence of base (confirmed by the ^{1}H NMR spectra in methanol-d_4), a mixture of varying ratio of the enol and DHOxyL$^-$ in presence of BA and TBA, and pure DHOxyL$^-$ with DBU (the identity of the ion in all cases was corroborated by selective excitations). As shown in Figure 7 by comparing the spectra of DHOxyLH in four short-chain alcohols (whose polarity decreases in the order methanol > ethanol > 1-butanol > 2-propanol), the polarity of the solvents affects the acid−base equilibrium. In all these solvents, the ground-state DHOxyLH existed as enol-DHOxyLH, with only traces of the ion present in more polar alcohols (methanol and ethanol). In absence of base, the absorbance (λ_{abs}^{max} = 361−362 nm) and emission (λ_{em}^{max} = 439−441 nm) maxima of the enol form remained almost invariable with the solvent. The dependence of the yield of the excited-state proton transfer on the solvent polarity, whereby (DHOxyLH)* is partially converted to (DHOxyL$^-$)*, followed by emission from the ion, can be well illustrated by the fluorescence spectra recorded in the absence of base. There, the

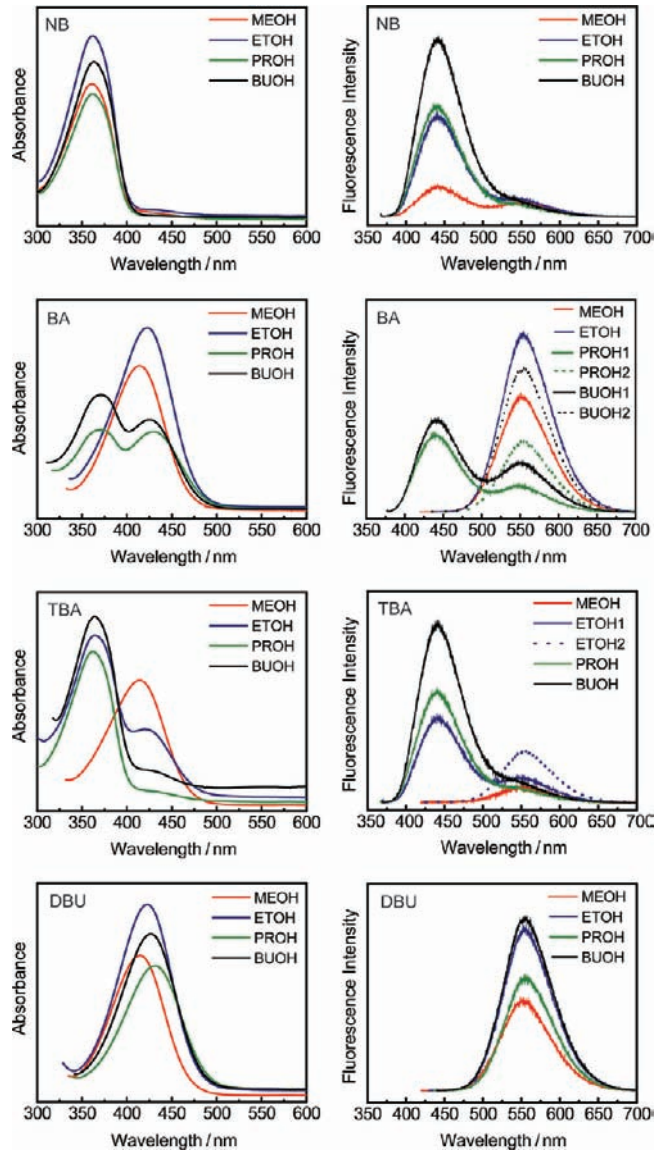

Figure 7. Absorption (left panels) and emission (right panels) spectra of DHOxyLH in alcohols. Solvents: MEOH, methanol; ETOH, ethanol; PROH, 2-propanol; BUOH, 1-butanol. Bases: NB, no base added; BA, butyl amine; TBA, tributyl amine; DBU, 1,8-diazabicyclo[5.4.0]undec-7-ene. The emission spectra recorded at second excitation wavelength are dotted (Table 3).

peak intensity of (enol-DHOxyLH)* decreased and the relative ratio of the two emission intensities λ_{max}^{em}(DHOxyL$^-$)/λ_{max}^{em}(enol-DHOxyLH) increased with increasing polarity. Actually, it appears that even a small difference in the basicity of the deprotonating agent, such as that between BA and TBA (ΔpK_a = 0.2), has a strong effect on the enol−enolate equilibrium (Figure 7). In the presence of the weaker base (TBA) in 1-butanol and 2-propanol, DHOxyLH exists mainly as enol-DHOxyLH, with only minor contribution from DHOxyL$^-$, and it is completely deprotonated only in the most polar solvent (methanol). In the case of the stronger base (BA), the relative concentrations of enol-DHOxyLH and DHOxyL$^-$ in 1-butanol and 2-propanol were similar, but in the two more polar solvents (methanol and ethanol), the compound was completely deprotonated. This result reflects the interplay between the polarity of a protic, polar solvent and the basicity of the proton acceptor in the protonation of the enol group of the ground-state chromophore. On the other hand, in presence of DBU in all

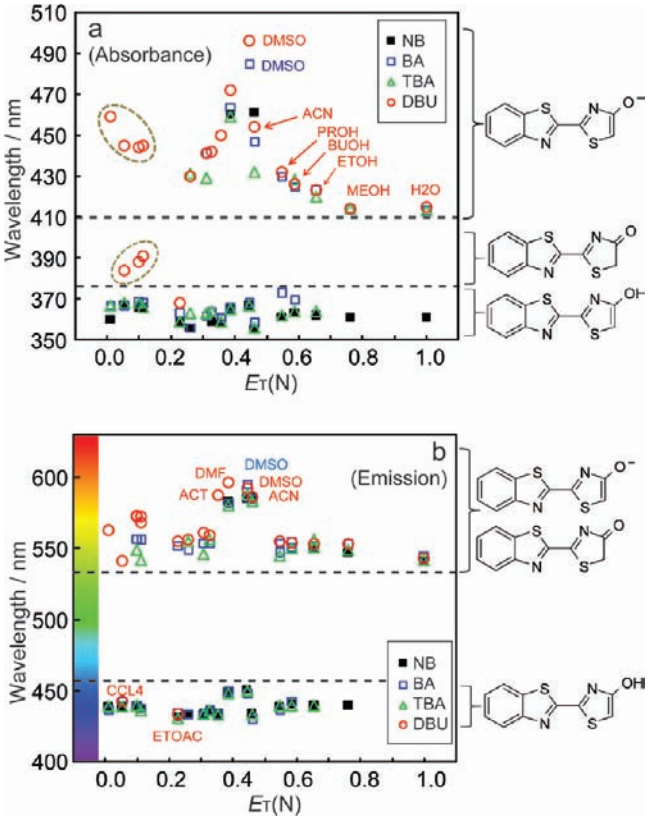

Figure 8. Dependence on the spectral maximum in the absorption (a) and emission (b) spectra on the E_T(N) values. The solvent abbreviations are given in the caption to Figure 4 (*m*-xylene was not included in the plot, due to unavailability of the respective parameters). Bases: BA, butyl amine; TBA, tributyl amine; DBU, 1,8-diazabicyclo[5.4.0]undec-7-ene.

four alcohols, the molecule was completely deprontonated in the ground state. The anion, however, showed larger variation of the absorption maximum with the solvent, and the values were inversely proportional to the solvent polarity: 414 nm (methanol) < 423 nm (ethanol) < 426 nm (1-butanol) < 432 nm (2-propanol). This effect appears as a result of the gradual change of the strength of the hydrogen bond DHOxyL$^-$···H−O(solvent) with the solvent polarity. The increased polarity of the protic solvents, therefore, results in decreased wavelength of the absorption of DHOxyL$^-$. At the same time, the emission energy of the pure ion (DHOxyL$^-$)* in DBU was practically unaffected by the solvent (553−555 nm), pointing out possible dissociation of the hydrogen bond between the emitter and the solvent in the excited state, followed by emission from the unbound ion. The shorter emission wavelength of the ion in alcohols (553−555 nm) relative to that in DMSO (592 nm) is probably a result of the competition for hydrogen bonding between enol-DHOxyLH and the solvent with DHOxyL$^-$.

2.2.3. Correlation of the Electronic Spectra with Solvent Polarity. Figure 8 shows the absorption and emission maxima of DHOxyLH in the studied solvents plotted against the normalized Dimroth−Reichardt's E_T(N) values,[69,70] which are usually considered a quantitative measure of the solvent−solute interactions inclusive of the specific solvent effects. Similar correlations have been employed previously to explain solvent effects on other bioluminescence emitters.[38,71] The plot of the wavelength at maximum absorbance (Figure 8a) shows three distinct regions that correspond to the absorption energies of enol-DHOxyLH (∼350−375 nm), keto-DHOxyLH (∼375−400 nm), and DHOxyL$^-$ (400−500 nm). Generally, DBU, which has better proton abstraction ability than the other two bases, provides conditions for wide energy distribution of the solvent-dependent absorption spectra, and it covers a wide region of the maximal absorbance; the color of the solution can be "tuned" over a range of 128 nm. When DBU is used, any of the three species can be created just by selecting the polarity of the solvent, but the keto form can only exist in nonpolar solvents. The DBU plot exhibits a λ-shaped curve, showing positive solvatochromism (increasing λ_{abs}^{max} with E_T(N)) in the region of aprotic solvents with low to medium polarity and a negative solvatochromism in the region of protic solvents with high polarity (alcohols and water), peaking at DMSO (E_T(N) = 0.444). In the low-polarity region, the plot is branched due to the coexistence, in the same solution, of the keto form (∼365−400 nm) and the ion (>400 nm). In the case of DBU, inspection of the region of ion emission (400−500 nm) shows that the enolate ion can be produced in all solvents that are more polar than ethyl acetate (E_T(N) = 0.228). With BA, the enolate ion exists in solvents that are more polar than DMF (E_T(N) = 0.386). Finally, with TBA, which is only marginally less basic than BA, the limiting polarity for creation of the ion is shifted to 1-butanol (E_T(N) = 0.586), so the ion can only exist in very polar solvents. As a consequence, in the vicinity of a strong proton acceptor, the ionization of the enol group in the ground state of the emitter may become possible even in a less polar environment. If the proton acceptor is weak, however, the proton transfer can occur only under very polar conditions. Thus, a polar environment can facilitate ionization of the enol group with a variety of basic moieties, whereas a less polar environment is more discriminative and requires strong base for deprotonation.

The plot of the fluorescence maxima against E_T(N) (Figure 8b) shows two regions, 430−450 nm and 540−600 nm, separated by a gap (450−540 nm). Based on the assignments detailed in the previous section, these ranges correspond to the emission from enol-DHOxyLH and keto-DHOxyLH/DHOxyL$^-$, respectively. The emission energies of the latter two species are close and their bands are overlapped. The selective excitation of keto-DHOxyLH and DHOxyL$^-$ absorption bands in nonpolar solvents, where both species coexist (benzene and toluene, in the presence of DBU, see Figure 5b), showed that the keto form emits at a lower wavelength than the ion. Therefore, while the enol form of DHOxyLH is a *blue-violet emitter*, the keto tautomer and the enolate ion are, respectively, *green* and *yellow-orange* emitters. The lowest-energy emissions (orange) are those from the DHOxyL$^-$ ion in DMF and DMSO in the presence of DBU (596 and 592 nm, respectively) and in DMSO in the presence of BA (595 nm). An important feature of the plot in Figure 8b is that the longest wavelength, and thus the lowest transition energy, was observed in solvents of medium polarity (DMSO and DMF), where the ions emit orange color. Unexpectedly, regardless of the strength of the base used to abstract the proton, the typical polar protic solvents, such as simple alcohols, result in blue shift of the emission band of the ion from the yellow to the green region. It can be concluded that, at least when the keto−enol−enolate equilibrium is considered,

(69) Reichardt, C. *Chem. Rev.* **1994**, *94*, 2319–2358.
(70) Reichardt, C. In *Solvents and Solvent Effects in Organic Chemistry*, 3rd ed.; Wiley-VCH: Weinheim, Germany, 2003.
(71) Hirano, T.; Takahashi, Y.; Kondo, H.; Maki, S.; Kojima, S.; Ikeda, H.; Niwa, H. *Photochem. Photobiol. Sci.* **2008**, *7*, 197–207.

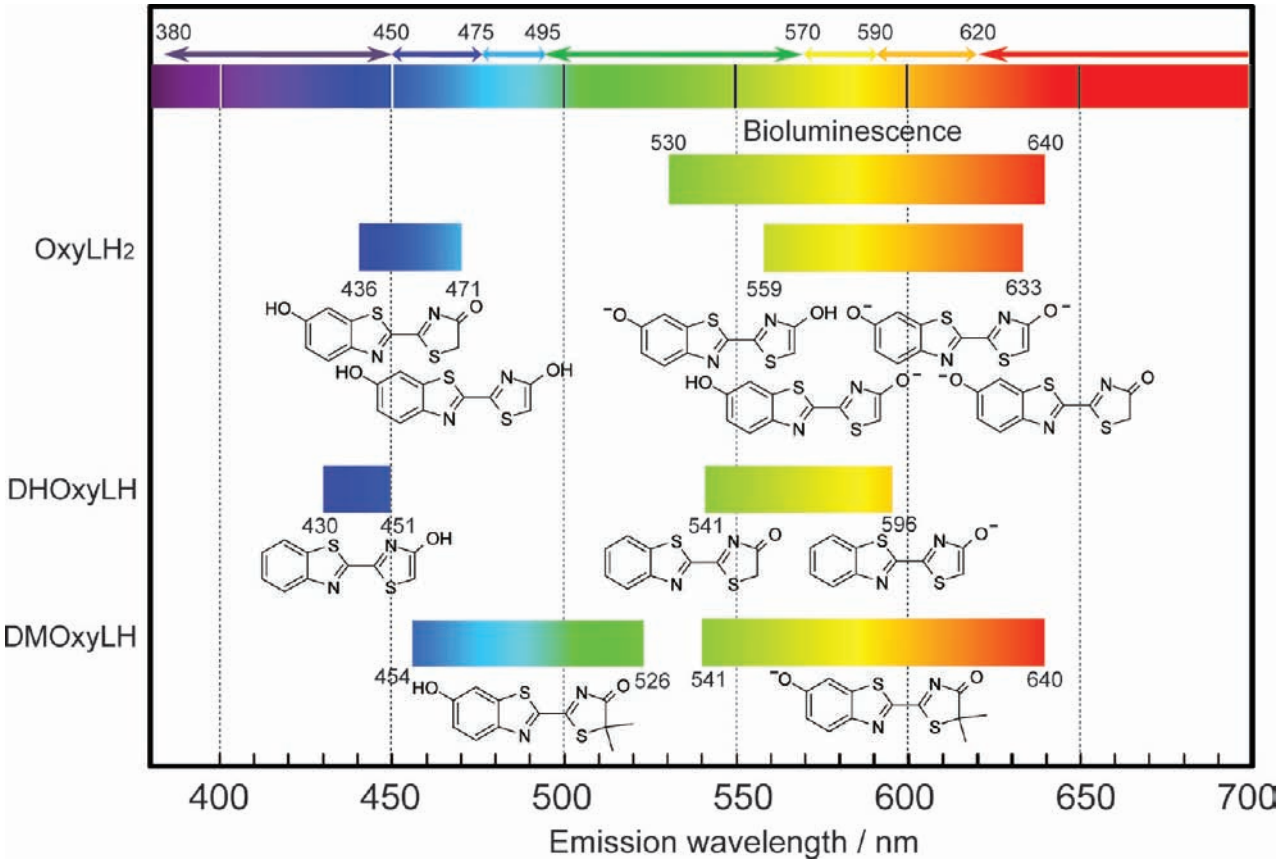

Figure 9. Color-coded emissive spectral regions of the natural bioluminescence, oxyluciferin ($OxyLH_2$),[41] 6′-dehydroxyoxyluciferin (DHOxyLH, this work), and dimethyloxyluciferin (DMOxyLH).[38] The data for $OxyLH_2$, DHOxyLH, and DMOxyLH were compiled from 7,[41] 18, and 8[38] solvents, respectively. In the case of deprotonated $OxyLH_2$ in methanol, we also observed emission at 463 nm, but that band was assigned to the neutral enol form. For DMOxyLH, the lowest emission in *p*-xylene and benzene was reported at 420 nm,[38] but the oscillator strength of that transition is very weak. The wavelength regions that correspond to the seven main colors from the visible spectrum (violet, blue, cyan, green, yellow, orange, and red) referred to in this study are marked in the spectrum on the top.

the strongest polarity does not necessarily result in the strongest red shift of the emission.

2.2.4. Substitution Effects on the Emission Spectra of DHOxyLH. Having the emission spectra of different forms of DHOxyLH assigned, these results can be employed to answer the questions posed in the Introduction. Figure 9 contains a schematic representation of the regions of the visible spectrum and the respective colors emitted by (DHOxyLH)* and its enolate anion in solvents of various polarity, compared with those reported for $(OxyLH_2)^*$[41] and (DMOxyLH)*,[38] and the spectrum of the natural firefly bioluminescence. The spectral changes that occur on going from $DHOxyLH_2$, the simplest emitter, to the other two molecules, allow direct insight into the spectroscopic consequences that each of the two functional groups has on the emission energy of the first excited state of $OxyLH_2$.

The width of the two spectral regions of DHOxyLH is notably narrower (430−451 nm, $\Delta\lambda_{em} = 21$ nm, and 541−596 nm, $\Delta\lambda_{em} = 55$ nm) relative to the other two emitters (436−471 nm, $\Delta\lambda_{em} = 35$ nm, and 559−633 nm, $\Delta\lambda_{em} = 74$ nm, for $OxyLH_2$; 454−526 nm, $\Delta\lambda_{em} = 72$ nm, and 541−640 nm, $\Delta\lambda_{em} = 99$ nm, for DMOxyLH). This is clearly an effect of the reduction of intramolecular excited-state charge transfer in DHOxyLH due to the absence of an electron-active substituent at the phenylene ring. Apparently, the 6′-OH/O^- group at the phenylene ring of $OxyLH_2$ and its ions is a *critical* prerequisite for the enhanced charge transfer, which widens the spectral range of the emitter while decreasing the emission energy to the orange-red region. In absence of the 6′-OH group, the red emission of $OxyLH_2$ would not be possible.

The emission wavelengths of the excited species derived from DHOxyLH are in the order (enol-DHOxyLH)* ≪ (keto-DHOxyLH)* ≤ $(DHOxyL^-)^*$. Spectral comparison of keto-DHOxyLH with keto-$OxyLH_2$ and DMOxyLH (the latter always being in the keto form) shows that the lowest λ_{em} shifts from 541 nm in DHOxyLH to 436 nm in $OxyLH_2$ and 454 nm in DMOxyLH. Thus, introduction of a neutral 6′-OH group in DHOxyLH strongly *blue shifts* the emission of the first excited state of the keto forms. Consequently, although (keto-DHOxyLH)* is a green emitter, (keto-$OxyLH_2$)* and (DMOxyLH)* are violet- or blue-emitting species. A similar, albeit less drastic, blue-shifting effect is seen from the 6′-hydroxylation on the enolate ion: whereas $(DHOxyL^-)^*$ is a yellow-orange emitter, $(enolate\text{-}OxyLH^-)^*$ is a yellow emitter. This is in agreement with the theoretical calculations[44] for $(enolate\text{-}OxyLH^-)^*$, which have predicted a maximum in the yellow region (580 nm) in DMSO solution. Contrary to the blue-shifting effect on the keto form and the enolate, the 6′-hydroxylation exhibits small *red shift* (20 nm, from 451 to 471 nm) of the high-wavelength emission edge of the enol form, so that both (enol-DHOxyLH)* and $(enol\text{-}OxyLH_2)^*$ are violet-blue emitters.

Probably as a consequence of the double electron-donating (methyl) substitution, which according to Chart 2 exerts significant effects on the structure of the thiazole ring,

(DMOxyLH)* (454−526 nm; $\Delta\lambda_{em} = 72$ nm) has a broader emission spectrum relative to (enol-$OxyLH_2$)* (436−471 nm; $\Delta\lambda_{em} = 35$ nm). The difference (55 nm) between their upper limits (451 and 526 nm) represents a measure of the effects that are due to the 5,5-dimethyl substitution. This effect of the methyl group on the emission energy needs to be taken into consideration when 5-methyl-substituted model molecules are utilized to study the emission properties of the real emitter.

Introduction of the *ionized* 6′-O^- group and thus a negative charge at the phenylene ring strongly perturbs the energy diagram of the emitter, decreasing the excited-state energy and *red shifting* the emission of all three species derived from DHOxyLH (Figure 9). For instance, (keto-DHOxyLH)*, a green-emitting species, becomes the red emitter phenolate−keto-OxyLH)*. A somewhat smaller red shift was observed for the yellow-emitting enolate form ($DHOxyL^-$)*, which becomes the orange-red emitter (Oxy^{2-})*. Similarly, whereas the enol form of DHOxyLH, (enol-DHOxyLH)*, emits blue light, (phenolate−enol-$OxyLH^-$)* is a green emitter. It should be noted that the strong red shift of the keto form caused by the 6′-O^- substitution may be further enhanced by resonance stabilization from the extended electron conjugation.[52] In the two limiting resonance structures, the negative charge can be localized on either the phenolate or the enolate oxygen atoms. This additional resonance stabilization of the keto−phenolate form causes switching of the relative order of energies of $OxyLH_2$, (phenolate−enol-$OxyLH^-$)* ≤ ($OxyL^{2-}$)* ≤ (phenolate−keto-$OxyLH^-$)*, relative to DHOxyLH, (enol-DHOxyLH)* ≪ (keto-DHOxyLH)* ≤ ($DHOxyL^-$)*.

Along the same lines of reasoning, the red shift caused by the 6′-O^- substitution of keto-DHOxyLH appears as a viable reason for the red shift observed with ($DMOxyL^-$)* (Figure 9). However, the red emission edge of the latter (640 nm), which is close to the lowest emission energy from $OxyLH_2$ (633 nm) and accidentally coincides with the lowest-energy emission of the natural bioluminescence, cannot be prescribed exclusively to the ionization of the 6′-OH group; as explained above, such a shift or widening of the emission spectrum of DMOxyLH is likely to be a cumulative result of several factors, including the contribution from the double methyl substitution.

3. Conclusions

In summary, the effects of environmental polarity on the enolization of the keto tautomer and on the deprotonation of the enol tautomer, as well as the possible role of the neutral or ionic 6′-hydroxyl group in the fluorescence of oxyluciferin, were assessed through a thorough study of the structure and absorption and fluorescence spectra of its 6′-dehydroxylated derivative. Although it is different from the real emitter of the firefly bioluminescence, this molecule provided a good model to separate the spectroscopic consequences of the presence of keto−enol−enolate and phenol−phenolate functional groups on the emission spectrum. The main conclusions of this model study are summarized below:

3.1. Spectroscopic Effects of the 6′-OH Group. The results from the spectroscopic analysis described in this work conform to the earlier studies, which have concluded that the two neutral (phenol) forms of oxyluciferin are blue-violet emitters (Figure 9). It is now clear that this is caused by the presence of a neutral 6′-OH group in such structures.

3.2. Spectroscopic Effects of the 6′-O^- Group. In accordance with the currently accepted mechanisms, we also confirmed that both green or red emission of oxyluciferin originates from its phenolate ion. The negative charge on the benzothiazole ring born by the 6′-O^- group is essential for effective charge transfer in the excited state, because it lowers the excited-state energy and red shifts the emitted light. In fact, the results from the model study presented here showed that in absence of a 6′-O^- group at the phenyl ring, it is not possible to obtain emission in the red region; being incapable of efficient excited-state charge transfer, such a molecule can only emit orange light. Moreover, we also showed that although the presence of a deprotonated 6′-O^- group is necessary, it is insufficient to account for the observed yellow-green and red emissions of the firefly oxyluciferin.

3.3. Effects of Solvent Polarity and Bases on the Enol Form. Polar or very polar environments stimulate the shift of the equilibrium toward the ground state of the enol form. Under such conditions, the enol group can be partly or completely deprotonated from the ground state or from the first excited state. The deprotonation of the ground-state enol form depends on the polarity of the solvent: a polar environment facilitates its ionization even in neutral solutions, while a less polar environment requires strongly basic conditions.

3.4. Effects of Solvent Polarity and Bases on the Keto Form. Without bases, the keto form can exist in the ground state only in solvents of very weak to medium polarity. In the presence of strong bases, the keto group can exist only in a nonpolar or very weakly polar environment, usually together with the enolate anion. The results also indicate that under such conditions, the keto group can be enolized and deprotonated in the excited state. It should be noted that, at least if the keto−enol−enolate equilibrium alone is being considered, the most polar solvents do not necessarily cause the strongest red shifts; instead, the environment of medium polarity is the most effective in decreasing the excited-state energy.

3.5. Relative Emission Energies of the Keto, Enol, and Enolate Forms. The critical role of the protonation state of the 6′-hydroxyl group in the oxyluciferin fluorescence is also reflected in the relative order of the maximum emission wavelengths of the three species involved in the keto−enol−enolate equilibrium: while in absence of the 6′-OH group it is enol ≪ keto < enolate, with a neutral 6′-OH group the order is keto < enol ≪ enolate, and with an ionized 6′-O^- group it is enol < enolate < keto. This switching of the excited-state energies is a combined result of several factors, including blue shift caused by the 6′-OH group, red shift caused by the 6′-O^- group, and additional stabilization by electron resonance of the phenolate−keto form.

3.6. Emission Spectrum of the Phenol−Enolate Form. We found that the phenol−enolate form of oxyluciferin, a species that probably exists only in mixtures with other forms of oxyluciferin and could not be experimentally detected in the previous studies, is a yellow emitter.

3.7. Implications for the Origin of the Red Emission from Oxyluciferin. In the most recent model for the mechanism of the emission color tuning,[38] the red emission from DMOxyLH was explained as a combined effect of the nature of the 6′-O^- group bonding to the cation and the solvent polarity through the interaction of the solvent with the keto group. Here, on DHOxyLH as a model, we have demonstrated that even in the absence of the 6′-O^- group, and thus without interaction with the cation, the enolate form can emit orange light. Introduction of the 6′-O^- in the keto and enolate forms strongly decreases the excited-state energy and red shifts the emission, so in the case of ionic oxyluciferin they emit in the orange and red regions

(Figure 9). This effect, however, is much more pronounced in the keto form, apparently as a result of the resonance stabilization. In effect, the emission wavelength order enol ≪ keto < enolate in the absence of 6′-OH switches to enol < enolate < keto with 6′-O^-. In that respect, our results are in accordance with the suggested red emission from the phenolate−enolate or phenolate−keto[51,52] forms.

4. Experimental Section

4.1. Materials, Synthesis, and Characterization. DHOxyLH was synthesized as an orange powder according to a procedure by Suzuki and Goto.[61] A small amount of crystals for XRD analysis was obtained by slow evaporation of a solution in MeOH above $CaCl_2$ under nitrogen (crystals obtained from acetone had identical unit cell parameters to those from MeOH). Elemental Anal. $C_{10}H_6N_2OS_2$, calcd/found: C 51.28/51.35, H 2.58/2.79, N 11.95/11.53. D(−)-LH_2 (Wako), AMP (TCI), and ATP (Chameleon) were obtained as commercial products. Crystals of D(−)-LH_2 were obtained by slow evaporation of methanol solution onto a siliconized glass at RT. $DMLH_2$ was prepared from 2-cyano-6-hydroxybenzothiazole (98.2%; Sequoia) and D(−)-penicillamine (Sigma) and characterized by ^{1}H NMR. To prepare DHDMOxyLH, 84 mg of the compound was dissolved in DMSO (7.5 mL), and 0.5 M *t*-BuOK in DMSO (142.5 mL) and isopropanol (0.6 mL) were added to the solution, whereupon green fluorescence was observed over a few minutes. After the solution was stirred 50 min at RT, an excess of dry ice was added, and the solvent was evaporated under vacuum with heating, affording a red liquid. The solid residue was extracted with MeOH, and after removal of the solvent under vacuum, six components were separated by preparative TLC (silica gel, MeOH/water 1:1, extraction with acetone): $R_f = 0$ (red), 0.04 (colorless), 0.73 (colorless), 0.88 (orange), 0.92 (red). Red crystals of DHDMOxyLH ($R_f = 0.88$) were obtained from a mixture of MeOH/acetone/DMSO. The ^{1}H NMR spectra were recorded from freshly prepared solutions with a Varian UNITY INOVA600 instrument operating at 600 MHz. Solvents were DMSO-d_6 (99.9%D; Sigma), MeOH-d_4 (99.8%D; Merck), $CHCl_3$-d_1 (99.8%; Merck), and ACN-d_3 (99.96%; Merck).

4.2. X-ray Diffraction Analysis. The RT X-ray diffraction data were collected in ω-scan mode with APEX2 diffractometer (Bruker AXS),[72] by using Mo Kα radiation from a rotating anode X-ray source, a confocal multilayer X-ray mirror and CCD detector. The integrated and scaled data[72] were corrected for absorption effects.[73] The structures were solved by using direct methods[74] and refined on F_o^2 with SHELXL.[75] The non-hydrogen atoms were treated anisotropically, and the aromatic, hydroxyl, and carboxyl hydrogen atoms were included as riding bodies. The water protons in the structure of D(−)-$DMLH_2 \cdot H_2O$ were refined from the electron density map, but their distances were constrained. The worse than optimum refinement statistics in the case of DHOxyLH is due to the low quality of the crystal; the data represent the best out of measurements on several samples.

4.3. Spectroscopy. The UV−visible absorption spectra were recorded on an Agilent-8453 photodiode array spectrophotometer. The spectra were recorded without addition of base (NB), or with butyl amine (BA), tributyl amine (TBA), or 1,8-diazabicyclo[5.4.0]-undec-7-ene (DBU). The concentration of the diluted solutions (Tables 2 and 3) was adjusted to optimize the maximum absorbance in the 200−700 nm region. The fluorescence spectra were recorded on a Shimadzu-RF5300PC spectrofluorophotometer. The emission spectra were recorded after exciting the solutions (ca. 1.5 μM) at the wavelength of maximum absorption in the respective solvent. The dependence of the UV−visible absorption spectrum of DHOxyLH on the pH (25 °C) was recorded from phosphate buffer solutions with pH of 6.00, 6.20, 6.40, 6.60, 6.80, 7.00, 7.20, 7.40, 7.60, 7.80, 8.00, 8.24, 8.40, 8.64, 8.80, and 9.00, using saturated solutions of DHOxyLH in water as the working solution. To record the fluorescence spectra, 4-fold dilution of the solutions was used, and the samples were excited at 380 nm.

Acknowledgment. We thank Prof. S. Fukuzumi and Dr. K. Ohkubo (Osaka University) for kindly making available the spectroscopy equipment. The financial support from the Japanese Science and Technology Agency, JST (FRBforGYR research program), is gratefully acknowledged.

Supporting Information Available: Crystallographic data in CIF format, IR spectra, absorption and emission UV−visible spectra, and NMR spectra. This material is available free of charge via the Internet at http://pubs.acs.org.

JA102885G

(72) *APEX2* (Ver. 2.1−4) and *SAINT* (Ver. 7.34A); Bruker AXS Inc.: Madison, WI, 2007.

(73) Sheldrick, G. M. *SADABS*; University of Göttingen: Göttingen, Germany, 1996.

(74) Altomare, A.; Cascarano, G.; Giacovazzo, C.; Guagliardi, A.; Burla, M. C.; Polidori, G.; Camalli, M. *J. Appl. Crystallogr.* **1994**, *27*, 435–436.

(75) Sheldrick, G. M. E. *SHELXL-97*; University of Göttingen: Göttingen, Germany, 1997.